Surface Rheology and Adsorption Kinetics Reveal the Relative Amphiphilicity, Interfacial Activity, and Stability of Human Exchangeable Apolipoproteins

Victor Martin Bolanos-Garcia,* Anne Renault,† and Sylvie Beaufils†
*Department of Biochemistry, University of Cambridge, Cambridge CB2 1TN, United Kingdom; and †Groupe Matiere Condensee et Materiaux, Universite de Rennes 1, Campus de Beaulieu, 35042 Rennes cedex, France

ABSTRACT Exchangeable apolipoproteins are located in the surface of lipoprotein particles and regulate lipid metabolism through direct protein-protein and protein-lipid interactions. These proteins are characterized by the presence of tandem repeats of amphiphatic α-helix segments and a high surface activity in monolayers and lipoprotein surfaces. A noteworthy aspect in the description of the function of exchangeable apolipoproteins is the requirement of a quantitative account of the relation between their physicochemical and structural characteristics and changes in the mesoscopic system parameters such as the maximum surface pressure and relative stability at interfaces. To comply with this demand, we set out to establish the relations among α-helix amphiphilicity, surface concentration, and surface rheology of apolipoproteins ApoA-I, ApoA-II, ApoC-I, ApoC-II, and ApoC-III adsorbed at the air-water interface. Our studies render further insights into the interfacial properties of exchangeable apolipoproteins, including the kinetics of their adsorption and the physical properties of the interfacial layer.

INTRODUCTION

Exchangeable apolipoproteins are found in higher organisms where they play a central role in the regulation of lipid exchange and remodeling. Members of this family are ApoA-I, ApoA-II, ApoA-IV, ApoA-V, ApoC-I, ApoC-II, ApoC-III, and ApoE. Human ApoA-I is a protein of 243-amino acid residues that is significantly associated with high-density lipoprotein (HDL) particles. ApoA-I promotes cellular cholesterol efflux (1) and interacts with several proteins such as the scavenger receptor class B type I (2) and the ATP-binding cassette transporter A1 (3). ApoA-I also exhibits a protective effect on HDL against coronary artery disease (4) and is a potent activator of lecithin acyltransferase, the enzyme that catalyzes cholesterol esterification on HDL (5).

Human ApoA-II associates to form homodimers linked through a disulfide bridge (6) and forms heterodimers with ApoE and ApoH (7). ApoA-II down-regulates neutrophil activity in a similar fashion to ApoA-I (8) and impairs the antioxidant properties of paraoxonase in HDL particles (9). The quantification of an ApoA-II isoform has been proposed as a potential marker for prostate cancer (10), and mutations in the stop codon of the apoA-II gene, which result in a carboxyl-terminal peptide extension of 21 amino acid residues, appear to be responsible for renal amyloidosis (11).

Human apolipoprotein ApoC-I plays a crucial role in the regulation of apolipoprotein E/β-VLDL particle interaction, quilomicron uptake, and inhibition of cholesteryl ester transfer protein (CETP) activity (12). ApoC-I has been associated with Alzheimer's disease (13), and there are indications that ApoC-I polymorphism represents a genetic risk factor for dementia and for cognitive impairment in the elderly (14). ApoC-I also accounts for protection from obesity and insulin resistance (15), apoptosis of aortic smooth cells (16), and lipoprotein clearance (17). ApoC-II activates lipoprotein lipase and is therefore central for lipid transport in blood (18). ApoC-III, the most abundant C apolipoprotein in human plasma, stimulates CETP activity (19) and regulates plasma triglyceride metabolism (20). In patients with type 1 diabetes, ApoC-III induces increased cytoplasmic free intracellular Ca^{2+} concentration and β-cell death (21).

The largest apolipoproteins, ApoA-I and ApoE, display a repeating pattern of homologous 11- and 22-mer amphipathic α-helical segments that are delineated by proline residues (22). In comparison, little is known about the structures of ApoA-IV and ApoA-V, which are also large members of this protein family. Computational analysis suggests that the α-helical regions of ApoA-IV are composed of homologous repeating 11- or 22-mer units, but those of ApoA-V are organized in discrete independently folded domains (23). In contrast to ApoA-I, ApoA-IV, and ApoE, the three ApoC apolipoproteins do not form an intramolecular helix-bundle domain but, rather, a linear arrangement of amphipathic α-helices (22).

The diversity of functions of exchangeable apolipoproteins involves their physical contact with lipids and proteins, including other apolipoproteins. The interaction of apolipoproteins with lipids present in the surface of lipoprotein particles inhibits the activity of transfer proteins such as CETP (24). However, it has been shown that the interaction between ApoA-I and ApoA-II regulates the binding of HDL to cells (25), that ApoC-I is able to displace ApoE from β-VLDL particles (26), and that the masking of the receptor domain of ApoB by ApoC-III inhibits the binding to LDLR (27).

Submitted June 15, 2007, and accepted for publication October 10, 2007.

Address reprints requests to Sylvie Beaufils, Université de Rennes 1. Bat 11A, Campus Beaulieu, 35042 Rennes cedex, France. E-mail: sylvie.beaufils@univ-rennes1.fr.

Editor: Kathleen B. Hall.

0006-3495/08/03/1735/11 $2.00

doi: 10.1529/biophysj.107.115220

Several studies on isolated apolipoproteins at interfaces have been reported in recent years (28–33). However, it has been difficult to evaluate with certainty the relative surface activity of these proteins for various reasons: 1), the exact locations and boundaries of the α-helices of various apolipoproteins were determined with certainty until very recently; 2), different studies reported different amphiphilicity scales for amino acid residues; and 3), the diversity of experimental conditions such as pH, temperature, protein concentration, and subphase composition involved in those studies makes bona fide comparisons among apolipoproteins difficult. Hence, we set out to establish the adsorption kinetics, stability, and rheology of exchangeable apolipoproteins at air-water interfaces using state-of-the-art techniques such as surface rheology and null-ellipsometry coupled to Brewster angle microsocopy (BAM). We establish that the surface activity of exchangeable apolipoproteins increases as follows: ApoA-I, ApoA-II, ApoC-I, ApoC-II, and ApoC-III and that the kinetics of adsorption, surface rheology, and stability correlate well with the amphiphilicity of α-helix segments. We anticipate that the same physicochemical properties that rule the adsorption of exchangeable apolipoproteins onto monolayers also govern their adsorption onto the surface of lipoprotein particles.

MATERIALS AND METHODS

Materials

All of the oligonucleotides described in this work were synthesized in the Protein and Nucleic Acid Chemistry facility at the Department of Biochemistry, University of Cambridge, UK. All polymerase chain reactions (PCR) were performed with PfuTurbo DNA polymerase (Stratagene, Stratagene Europe, Amsterdam, The Netherlands) using a PTC-100 Thermal Cycler (MGE,). The amplicon was cloned in a pRSET-A vector (Invitrogen, Carlsbad, CA) under control of the T7 promoter. This vector also contains the encoding sequence of a tandem of six N-terminal histidine residues followed by a thrombin cleavage site (GLVPRG). The identity of recombinant ApoC-I was confirmed by mass spectrometry (MALDI-TOF) and N-terminal sequence analysis according to the Edman degradation technique. Human TPR-PP5(16-181) and ApoC-I were expressed in *E. coli* BL21 Codon plus. BUB1 and BUBR1 protein constructs were expressed in *E. coli* BL21 (DE3) as GST fusions. Both bacteria strains were from Stratagene (La Jolla, CA). Human apolipoproteins ApoA-I, ApoA-II, ApoC-I, ApoC-II, and ApoC-III isolated from human serum and of a purity of ~90% were obtained from Calbiochem (Calbiochem, Merck Chemicals Ltd. Nottingham, UK). Expression vector pGEX4T-1, high-purity thrombin, and the chromatography columns XK 26, Superdex 75 Hiload 26/60, Sepharose glutathione fast flow, and benzamidine fast flow were obtained from Amersham Pharmacia (Uppsala, Sweden). Ni-NTA resin was from Qiagen (West Sussex, UK). Tablets of a cocktail of protease inhibitors were from Boehringer Mannheim (Roche Diagnostics, East Sussex, UK). A French press was used for cells rupture (SIM-Aminco, Rochester, NY). Benzamidine, imidazole, and all the salts used for preparing buffer solutions were obtained from Sigma (St. Louis, MO). Buffer and protein solutions were prepared with ultrapure water (Nanopure-UV, Barnstead, Dubuque, IA). Dialysis was carried out using a regenerated cellulose dialysis membrane of 3500 MWCO (Spectra/Por; Spectrum Lab., Rancho Dominguez, CA). Quartz cells for circular dichroism (CD) were from Hellma (Essex, UK).

Methods

Synthesis of the ApoC-I encoding sequence

The set of overlapping oligonucleotides designed for the synthesis in vitro of the full-length, human ApoC-I encoding sequences were named as follows: Oligo apoC1-1: 5′ GTATGCTGTCACGGATCCACCCCAGACGTCTCCAGCGCCTTGGATAAGCTGAAGGAGTTTGGTAC 3′; Oligo apoC1-2: 5′ TAGTTGAGGTCCGAATTCTTAT TAAGAGTCAATCTTGAGTTTCTCCTTCACTTTCTGAAATGTCT 3′; Oligo apoC1-3: 5′ TGAGTTTCTCCTTCACTTTCTGAAATGTCTCAGAAAACCACTCA CGCATCTTGGCAGAAAGTTCGCTCTGTTTGATGCGGCTGATG 3′; Oligo apoC1-4: 5′GGATAAGCTGAAGGAGTTTGGTAACACACTGGAGGACAAGGC TCGTGAACTCATCAGCCGCATCAAACAGAGCGAACTTTCT 3′; Oligo apoC1-5: 5′ GTATGCTGTCACGGATCCACCCCAGACGTCTCTAGC 3′; Oligo apoC1-6: 5′ TAGTTGAGGTCCGAATTCTTATTAAGAGTCAATCTT 3′; Oligo apoC1-7: 5′ GTATGCTGTCACGGATCCACCCCAGACGTCTCTAGC 3′; and apoC1-8: 5′ TAGTTGAGGTCCGAATTCTTATTAAGAGTCAATCTT 3′. Some minor modifications were introduced into the original human encoding sequence to optimize its expression according to the preferential codon usage in *E. coli*. Nested PCR was carried out for the synthesis of the human ApoC-I encoding sequence according to the following PCR program: segment 1, 30 s at 95°C; segment 2, 1 min at 55°C, and segment 3, 4 min at 68°C, 18 cycles. The pRSET-A vector was double-digested with the restriction enzymes *Bam*HI and *Eco*RI to clone the tailored human ApoC-I encoding sequence immediately downstream from the codons encoding for the residues HHHHHHGLVPRG.

Protein expression and purification

Recombinant ApoC-I was expressed using conventional protocols. Briefly, cells were grown at 37°C, 250 rpm in 2× TY broth containing ampicillin. Induction was done using IPTG at cell densities of 0.6–0.8 $OD_{600\ nm}$. Inclusion bodies were resuspended in denaturing buffer (i.e., Tris buffer 20 mM containing 8 M urea, 25 mM imidazole, and 5 mM β-mercaptoethanol, pH 8.0), and 100 ml of denaturing buffer was used per 2 g of inclusion bodies. The resulting solution was loaded onto an XK 26 column packed with 12 ml of Ni-NTA agarose previously equilibrated in the same buffer solution. After being washed with ~20 column volumes, recombinant ApoC-I was refolded into the column, concentrated, loaded onto a gel filtration column (Superdex 75, HR 26/60), and eluted in 20 mM Tris buffer, 200 mM NaCl, pH 8.0 (TBS buffer) at 1 ml/min. After analysis by SDS-PAGE and measurement of UV absorption spectra (200–300 nm), fractions containing pure ApoC-I were collected and concentrated. Refolded ApoC-I was subjected to thrombin cleavage after extensive dialysis in TBS. One unit of thrombin protease of high purity was used to digest 1 mg of recombinant ApoC-I at 4°C overnight. Thrombin and the cleaved histidine tag were removed using a benzamidine fast flow column and a Ni-NTA column, respectively, previously equilibrated in TBS. Pure recombinant ApoC-I was concentrated fivefold and dialyzed several times against 4 liters of dialysis buffer (20 mM ammonium bicarbonate buffer, pH 8.0), lyophilized, and stored at −20°C. N-terminal sequence and mass spectrometry were carried out to confirm protein identity and purity of recombinant ApoC-I.

Every protein described in this study was subjected to gel filtration chromatography (Superdex 75, HR 26/60; TBS buffer as the mobile phase) to remove any oligomer of high molecular mass and to maintain protein samples in the same buffer solution. In all of the cases, gel filtration chromatography was performed immediately before experiments in monolayers.

Ellipsometry and BAM

Monolayers were prepared on a circular trough ($S = 20\ cm^2$), and the surface pressure was measured with a sensor (Nima Technology, Coventry, UK) using a Wilhelmy plate. The ellipsometric measurements were carried out

with a home-made ellipsometer (34) operated with He–Ne laser ($\lambda = 632.8$ nm, Melles Griot, Carlsbad, CA) that was polarized with a Glan-Thompson polarizer. The incidence angle of the light on the surface was 1° away from the Brewster angle. After reflection on the water surface, the laser light passed through a $\lambda/4$ retardation plate, a Glan-Thompson analyzer, and a photomultiplier. Through a computer-controlled feedback loop, the analyzer automatically rotated toward the extinction position. In this ''null ellipsometer'' configuration (35), the analyzer angle, multiplied by 2, yielded the value of the ellipsometric angle (Δ), i.e., the phase difference between parallel and perpendicular polarization of the reflected light. The laser beam probed a surface of 1 mm^2 and a depth of the order of 1 μm. The ellipsometric angle Δ is proportional to the quantity of protein adsorbed at the interface in the case of a monolayer. Hence, the variation of the ellipsometric angle is a relevant probe for changes occurring at the interface. By use of the measured ellipsometric angle, Δ, and an estimate of the refractive index increment of the protein to 0.2 ml/g, the surface concentration Γ of adsorbed protein was calculated using the relation between Δ and Γ reported by De Feijter et al. (36). Initial values of the ellipsometric angle (Δ_0) and surface tension of pure buffer solutions were recorded on the subphase for at least a half-hour. These values have been subtracted from all data presented below. Values of Δ and surface pressure (π) were stable and recorded every 4 s with a precision of $\pm 0.5°$ and ± 0.5 mN/m, respectively. BAM was performed in a homemade device with a spatial resolution ~ 4 μm. In this setup, the interface is illuminated at the Brewster incidence ($\cong 53°$) with a polarized beam from a He-Ne laser. A microscope receives the reflected beam and the signal transmitted to a CCD video camera to develop an image of the monolayer. Protein concentrations used for ellipsometry, surface pressure measurements, and BAM observations were in the range 1–80 μg/ml in 20 mM sodium phosphate buffer, pH 7.0.

Surface rheology

The principles and implementation of our experimental setup for the measurement of the lateral rigidity of monolayers and the procedure for data analysis have been extensively described before (37,38). Briefly, at the center of a 48-mm-diameter Teflon trough, a 10-mm-diameter paraffin-coated aluminum disk floats at the air-water interface, in contact with the monolayer whose rigidity is measured. The subphase is 5 mm deep. The float carries a small magnet and is kept centered by a permanent magnetic field, $B_0 = 6 \times 10^{-5}$ T, parallel to the Earth's field and created by a small solenoid located just above the float. Sensitive angular detection of the float rotation is achieved using a mirror fixed on the magnet to reflect a laser beam onto a differential photodiode. A sinusoidal torque excitation is applied to the float in the 0.01- to 100-Hz frequency range by an oscillating field perpendicular to the permanent solenoid field. The latter field acts as a restoring torque equivalent to a monolayer with a rigidity of 0.16 mN/m. This number set the sensitivity limit of the rheometer. The device behaves as a simple harmonic oscillator. The resistance that the monolayer opposes to the rotation of the float is directly measured. An important advantage of this setup is the absence of physical link between the outside and the float torsion (i.e., no torsion wire). This allows high sensitivities such that the applied deformation is very small, below $\boldsymbol{u}_{xy} \approx 10^{-7}$ where $\boldsymbol{u}_{xy}$ corresponds to the deformation tensor. This device introduces very small excitation strains (from 10^{-3} down to 10^{-6}) to the system. Because in previous experiments we have shown that pure shear elastic response spectra exhibit a linear stress-strain relation over this range (37), we concluded that the rotation coupling between the float and the contacting monolayer is satisfactory. Moreover, we have shown that such small strains do not create plastic deformations on fragile surface objects (38).

For the experimental procedure, the amplitude and phase of the mechanical response of the pure subphase were first analyzed in the frequency range 0.01–100 Hz to establish that no rigidity was detected. This measurement takes approximately 1 h. Then, the protein solution was directly poured in the trough, and the mechanical response of the layer formed at the interface was recorded at the fixed frequency of 5 Hz. At the end of the adsorption kinetics, when the shear elastic constant, μ (expressed in mN/m) reached a constant value, a new measurement between 0.01 Hz and 100 Hz was recorded to determine whether the system behaves as an elastic layer. Rigidity measurements were carried out in parallel to ellipsometry. All of the experiments were performed at 18°C.

RESULTS

Expression and purification of the human ApoC-I encoding sequence

Single nucleotide substitutions introduced in the synthetic ApoC-I encoding sequence to avoid the problem of codon bias were adequate as ApoC-I was overexpressed in the eubacteria *E. coli*, and the amino acid sequence of this protein was confirmed to be identical to that deposited in the Entrez Protein database (Access number P02654). Recombinant human ApoC-I thus expressed formed inclusion bodies but was efficiently refolded when bound to metal affinity chromatography columns. The strategy used consists of a decrease of urea concentration (typically from 6 M to 5 M) followed by a fast increase from 5 M to 5.5 M; then, a second decrease (from 5.5 M to 4.5 M), a new reincrease from 4.5 M to 5 M, and so on until urea was completely depleted from the column and replaced by 20 mM Tris buffer containing 10 mM β-mercaptoethanol, pH 8.0. Refolded recombinant ApoC-I and that isolated from human serum exhibited identical secondary structure content as determined by far-UV circular dichroism (data not shown). Previous reports on the CD spectroscopy analysis of several exchangeable apolipoproteins, including ApoC-I (39), ApoA-II (40), ApoA-I, and ApoC-III (31), have shown that these proteins do not show a concentration-dependent signal in the concentration range 10^{-7} M to 10^{-6} M. In addition, dynamic light-scattering studies on ApoA-I self-association have shown that this protein can form oligomers of higher organization at concentrations above 1 mg/ml (41).

Exchangeable apolipoproteins form stable monolayers

The molecular mass of exchangeable apolipoproteins varies as follows: ApoC-I, 6.6 kDa; ApoC-III, 8.7 kDa; ApoC-II, 8.9 kDa; ApoA-II, 17 kDa; and ApoA-I, 28 kDa. Solutions of ApoA-I at molar subphase concentrations ranging from 10^{-8} M to 10^{-6} M and of ApoA-II, ApoC-I (native and recombinant), ApoC-II, and ApoC-III at concentrations of 10^{-7} M and 10^{-6} M were used to characterize the interfacial properties of these proteins under identical experimental conditions. As shown in Fig. 1 *A*, exchangeable apolipoproteins rapidly adsorb at the interface (less than 20 min at the same subphase concentration of 10^{-6} M), leading to a maximal surface pressure between 22 to 26 mN/m. Not surprisingly, recombinant ApoC-I and that isolated from human serum exhibited similar adsorption kinetics (see inset of Fig. 1). For this reason, in the following sections only the series of studies conducted on recombinant ApoC-I are

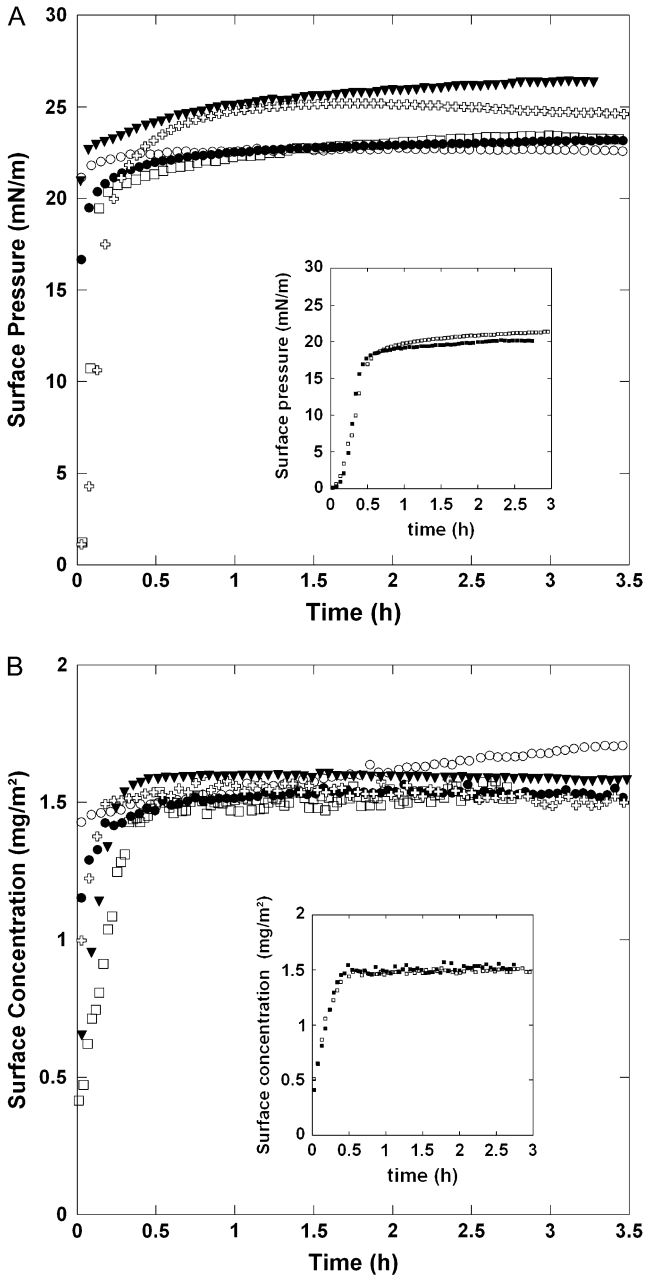

FIGURE 1 (*A*) Surface pressure and (*B*) surface concentration (referred to as Γ_{max}) as a function of time of exchangeable apolipoproteins at the subphase concentration of 10^{-6} M. Open squares, ApoC-I; open circles, ApoA-I; solid circles, ApoA-II; solid triangles, ApoC-III; crosses, ApoC-II. (*Insets*) Comparison of native (*open squares*) and recombinant (*solid squares*) ApoC-I at the subphase concentration of 10^{-7} M.

presented. Null ellipsometry measurements recorded at the same molar subphase concentration (i.e., 10^{-6} M) indicated that similar amounts of ApoA-I, ApoA-II, ApoC-I, ApoC-II, and ApoC-III were adsorbed at the air-water interface (i.e., $\sim 1.5 \pm 0.25$ mg/m^2) (Fig. 1 *B*). However, the time necessary to reach the interface and form a stable layer greatly varied among exchangeable apolipoproteins: for ApoC-I it was 30 min; for ApoA-I, 1 min; ApoA-II, 15 min; ApoC-II, 15 min; and ApoC-III, 25 min. Consistent with null ellipsometry measurements, direct BAM observations showed that ApoA-I, ApoA-II, ApoC-I, ApoC-II, and ApoC-III were rapidly adsorbed at the interface and formed homogeneous layers at the BAM resolution (4 μm) (Fig. 2). The maximal surface concentration of these apolipoproteins (expressed in mg/m^2) is lower than that of small, all-α-helix protein domains containing other classes of tandem repeats such as the tetratricopeptide (TPR) motifs of human protein phosphatase 5 (PP5) (4.7 mg/m^2) and human BUBR-1 (3.5 mg/m^2) (42). In addition to being surface active, the direct comparison among these proteins is pertinent because the molecular masses of TPR-PP5 (19 kDa) and TPR-BUBR-1 (27 kDa) are approximately the same as those of ApoA-II and ApoA-I, respectively.

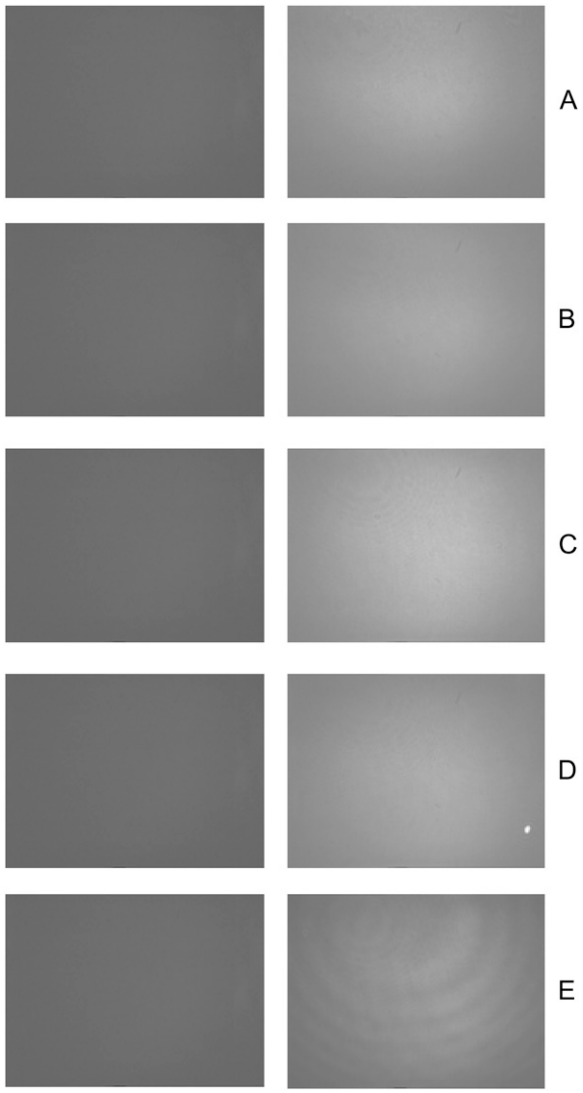

FIGURE 2 BAM images of exchangeable apolipoproteins at the air-water interface after 5 h of adsorption at the subphase concentration of 10^{-6} M. (*Left*) Control (buffer); (*right*) protein. (*A*) ApoC-I; (*B*) ApoA-I; (*C*) ApoA-II; (*D*) Apo-CIII; (*E*) ApoC-II.

The surface concentration, Γ_{max}, of exchangeable apolipoproteins was studied at the subphase concentrations of 10^{-6} M to estimate the number of molecules adsorbed at the interface (Fig. 3). As Fig. 3 shows, Γ_{max} (expressed in mol/m^2) seems to be inversely proportional to the molecular mass: the smallest proteins, ApoC-I, ApoC-II, and ApoC-III, show more molecules adsorbed at the interface than ApoA-I and ApoA-II.

The evolution of the surface pressure versus the subphase concentration for ApoA-I (Fig. 4) is typical of amphiphilic molecules: at low subphase concentrations, the surface pressure increases with subphase concentration up to a critical value for which the surface is saturated (43,44). Then, one of two scenarios can occur: 1), either the protein forms a stable interfacial monolayer and no more molecules adsorb beneath the interface (in which case the surface pressure and the ellipsometric angle are constant); or 2), additional molecules can adsorb in a reversible manner beneath the surface. In this case, the ellipsometric angle increases while the surface pressure remains constant (44). Our experiments do not shed light on which of the two processes takes place because ellipsometric measurements have not been performed on a wide subphase concentration range. However, we can assert that the surface is saturated because the surface pressure of ApoA-I (22 mN/m) does not depend on subphase concentrations above 10^{-7} M. For the other apolipoproteins, ellipsometric measurements have been carried out at the subphase concentrations of 10^{-7} M and 10^{-6} M. The surface pressure at the end of adsorption kinetics is nearly the same at these two subphase concentrations (Fig. 4, *inset*), suggesting that the plateau value of the surface pressure has been reached and the surface is saturated.

Kinetics of adsorption at interfaces

Adsorbed surface concentration and surface pressure were recorded at the low protein concentration of 3 μg/ml to follow the first adsorption events and to extract several parameters relevant to the surface activity. Two of these parameters were obtained from the plot of Γ versus π (Fig. 5). Here, Γ_0 is the surface concentration at which the surface pressure becomes different from zero. θ is extracted from the slope of the Γ-π curve (i.e., $\Delta\pi/\Delta\Gamma$) and corresponds to the increase of surface pressure relative to the increase of surface concentration (45).

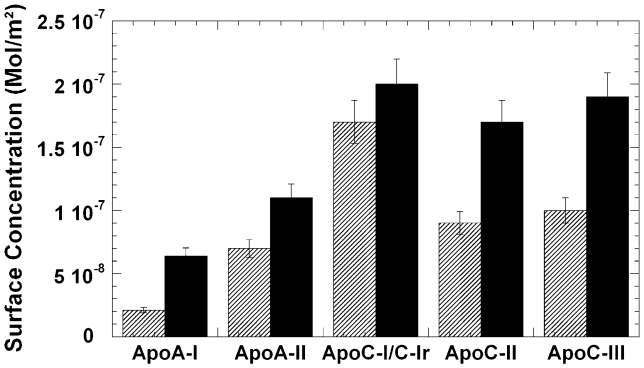

FIGURE 3 Apolipoprotein surface concentration (expressed in mol/m^2). Solid bars correspond to the maximal surface concentration (Γ_{max}) reached at the end of the adsorption kinetics at the subphase concentration of 10^{-6} M. Hatched bars correspond to Γ_0, the minimal surface concentration necessary to initiate surface pressure (see Fig. 5 for the determination of Γ_0).

In contrast to Γ_{max}, which is similar in all of the cases (expressed in mg/m^2), Γ_0 varies greatly: for ApoA-I, $\Gamma_0 = 0.6$ mg/m^2; ApoA-II, $\Gamma_0 = 1.2$ mg/m^2; ApoC-I, $\Gamma_0 = 1.1$ mg/m^2; ApoC-II, $\Gamma_0 = 0.8$ mg/m^2; and ApoC-III, $\Gamma_0 = 1.1$ mg/m^2 (Fig. 5). When the ratio Γ_{max}/Γ_0 is close to 1 (i.e., Γ_{max} is slightly higher than Γ_0), it suggests that as soon as the surface coverage is sufficient to initiate nonnull surface pressure, only a few more molecules adsorb onto the film. On the contrary, a higher Γ_{max}/Γ_0 ratio indicates that molecules find a place at the interface once the surface coverage has been initiated. This behavior can be attributed to protein conformational changes at the interface such that molecules occupy the remnant surface available. The ratio Γ_{max}/Γ_0 is equal to 2.7 in the case of ApoA-I (Fig. 3), which is comparable, under the same experimental conditions, to that of other surface-active proteins such as BUBR-1 and β-casein (42,46). This ratio is much lower for other exchangeable apolipoproteins (ranging between 1.9 and 1.2) and follows the decreasing order: ApoC-II > ApoC-III > ApoC-I > ApoA-II. Moreover, the high value of θ (higher than 33 mN·m/mg) compared with other surface-active proteins (45) indicates that extensive lateral interactions occur when the surface cover becomes effective (i.e., when $\Gamma > \Gamma_0$). This parameter further indicates that exchangeable apolipoproteins belong to a group of highly surface-active proteins.

In the first steps of adsorption kinetics at low bulk concentration, the transport of apolipoprotein molecules from the subphase to the interface is assumed to be a diffusion-controlled process. Therefore, the surface concentration Γ follows the relation of Ward and Tordai (47) (Eq. 1):

$$\Gamma = 2C_b(Dt/3.1416)^{1/2}, \quad (1)$$

where Γ is the surface concentration (mg/m^2), C_b is the subphase concentration (mg/m^3), and t the time (s). The initial part of the Γ-$t^{1/2}$ plot shows a linear correlation (Fig. 6), making possible the calculation of the diffusion coefficient, D. As shown in Table 1, ApoA-I, ApoA-II, ApoC-I, ApoC-II, and ApoC-III all have a diffusion coefficient of the same order of magnitude (i.e., of the order of 10^{-10} m^2/s) as that reported for other globular proteins of a similar size (36).

Surface rheology reveals the formation of rigid monolayers

The mechanical behavior of monolayers of exchangeable apolipoproteins at the air-water interface was investigated at

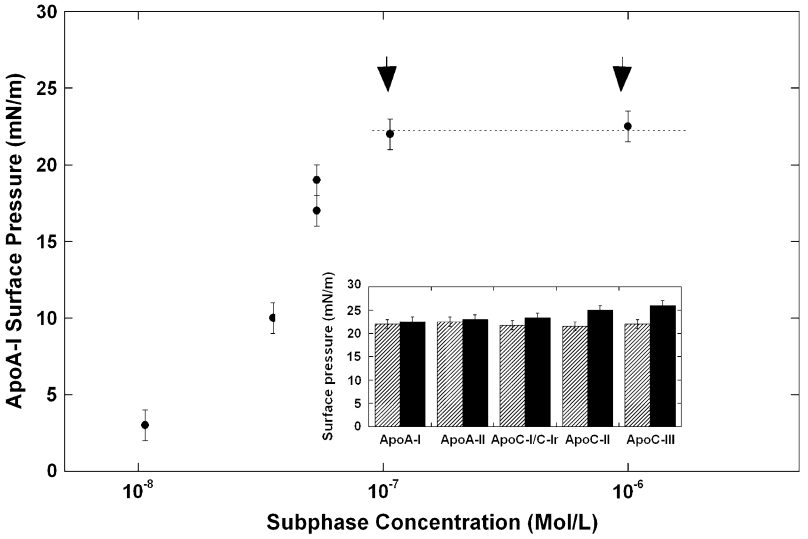

FIGURE 4 Surface pressure of ApoA-I reached at the end of the adsorption kinetics as a function of subphase concentration. (*Inset*) Surface pressure of other exchangeable apolipoproteins at the two subphase concentrations indicated by the arrows: 10^{-7} M (*hatched bars*) and 10^{-6} M (*solid bars*).

the fixed frequency of 5 Hz and subphase concentrations within the range 10^{-7}–10^{-6} M. Even at the lowest subphase concentration (i.e., 3 μg/ml), the final shear elastic constant, μ, reached high values. It is important to mention, for the fair comparison of the interfacial rheology of exchangeable apolipoproteins at the end of the adsorption kinetics, that triplicate experiments showed a variation of the absolute magnitude of this constant of up to 20%. Nevertheless, the study of the evolution of the shear elastic constant as a function of time clearly shows that molecules reaching the interface self-organize to form a cohesive layer (Fig. 7).

At the end of each adsorption kinetics (around 10 h, indicated by the *arrow* in Fig. 7), the amplitude and phase of the mechanical response of the monolayer were analyzed in the frequency range 0.01–100 Hz. For each exchangeable apolipoprotein, the real and imaginary part of the response adjusted well to an elastic layer model (i.e., a simple harmonic oscillator), as shown in the inset of Fig. 7. This indicates that medium- and long-range interactions play a major role in the cohesion of the layer. During the first hours, the kinetics of the formation of the interfacial layer is similar for all apolipoproteins. However, once the interfacial layer is formed, the interfacial behavior differs in each case: ApoC-II reaches a plateau around 22 mN/m over the first 5 h, which is

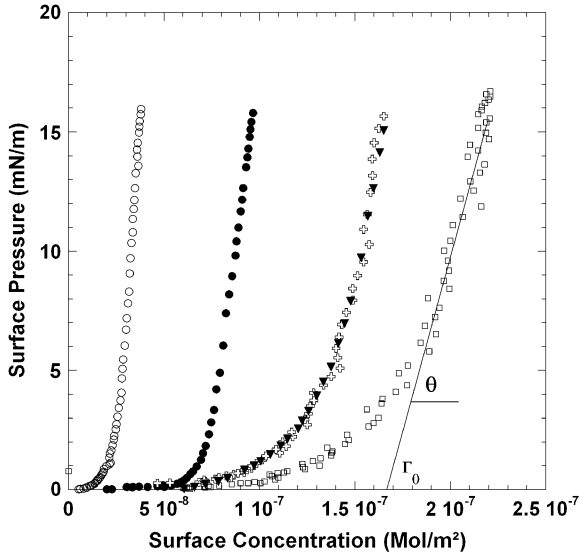

FIGURE 5 Estimation of Γ_0 and θ of exchangeable apolipoproteins calculated from the adsorption kinetics at the subphase concentration of 3 μg/ml, pH 7. (*Open squares*) ApoC-I; (*open circles*) ApoA-I; (*solid circles*) ApoA-II; (*solid triangles*) ApoC-III; (*crosses*) ApoC-II.

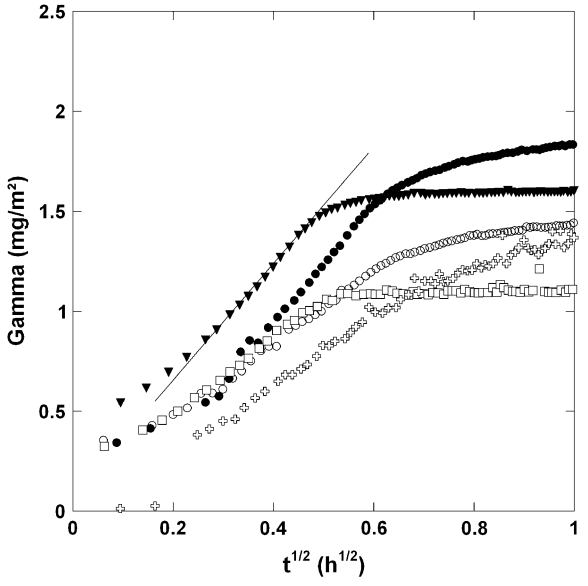

FIGURE 6 Surface concentration Γ (mg/m^2), as a function of the square root of time, $t^{1/2}$, ($h^{1/2}$). (*Open squares*) ApoC-I; (*open circles*) ApoA-I; (*solid circles*) ApoA-II; (*solid triangles*) ApoC-III; (*crosses*) ApoC-II. In the first part of the kinetic adsorption at low subphase concentration the process is diffusion controlled. Hence, the surface concentration obeys the law: $\Gamma = 2C_b(Dt/3.1416)^{1/2}$. The slope of the curve Γ versus $t^{1/2}$ (shown on the graph in case of ApoC-III) gives the value of the diffusion coefficient, D (m^2/s^{-1}).

TABLE 1 Comparison of the maximal surface pressure and rheological properties of exchangeable apolipoproteins

Protein	Max. surface pressure (mN/m)	Max. surface conc. (mg/m^2)	Diff. coeff. ($\times 10^{-10}$ m^2/s)	Max. μ after 15 h	θ (mN·m/mg)	Γ_0 (mol/m^2)
ApoA-I	22.5	1.6	0.9	22	40	$2.1\ 10^{-8}$
ApoA-II	23	1.5	1.8	48	33	$7\ 10^{-8}$
ApoC-I	23.5	1.5	1.5	38	41	$1.7\ 10^{-7}$
ApoC-II	25	1.5	0.4	12	37	$9\ 10^{-8}$
ApoC-III	26.5	1.5	6.3	28	41	$1\ 10^{-7}$

followed by a steady decrease of rigidity (about −6 mN/m over 6 h). In contrast, ApoA-I shows a plateau at ~20 mN/m up to 10 h, suggesting that no further major reorganization occurs in the monolayer. After the formation of the layer, the rigidity of ApoC-III increases slightly but regularly (~8 mN/m over 12 h), and ApoC-I and ApoA-II show a similar behavior: after initial adsorption, μ rapidly increases (~12 mN/m and 22 mN/m, respectively) and reaches a plateau after 8 h ($\mu = 38$ mN/m and 48 mN/m, respectively).

DISCUSSION

In previous reports (30,31), we have discussed the fact that the preferred protein conformations that exchangeable apolipoproteins adopt when deposited at the interface are those where the amphipathic α-helices lay horizontally on the aqueous subphase. Such interfacial organization permits these proteins to travel on a landscape of close energy minimum configurations (31,48). Indeed, recent studies on ApoA-I have shown that many (if not all) of the functions of lipid-free and HDL-bound ApoA-I arise from its various conformational states (49,50), whereas the three-dimensional structure of human ApoC-II in complex with sodium dodecyl sulfate (SDS) micelles has shown that flexibility of the C-terminal helix is required for the activation of lipoprotein lipase (18). Besides, the crystal structures of ApoA-I (51) and ApoA-II (52), the NMR structure of ApoC-I (53) and ApoC-II (54), as well as the structural model of ApoC-III (22) show that these proteins present few conformational constraints. These common features suggest that exchangeable apolipoproteins require a flexible and adaptable structure to carry out the multiplicity of their functions (22,55).

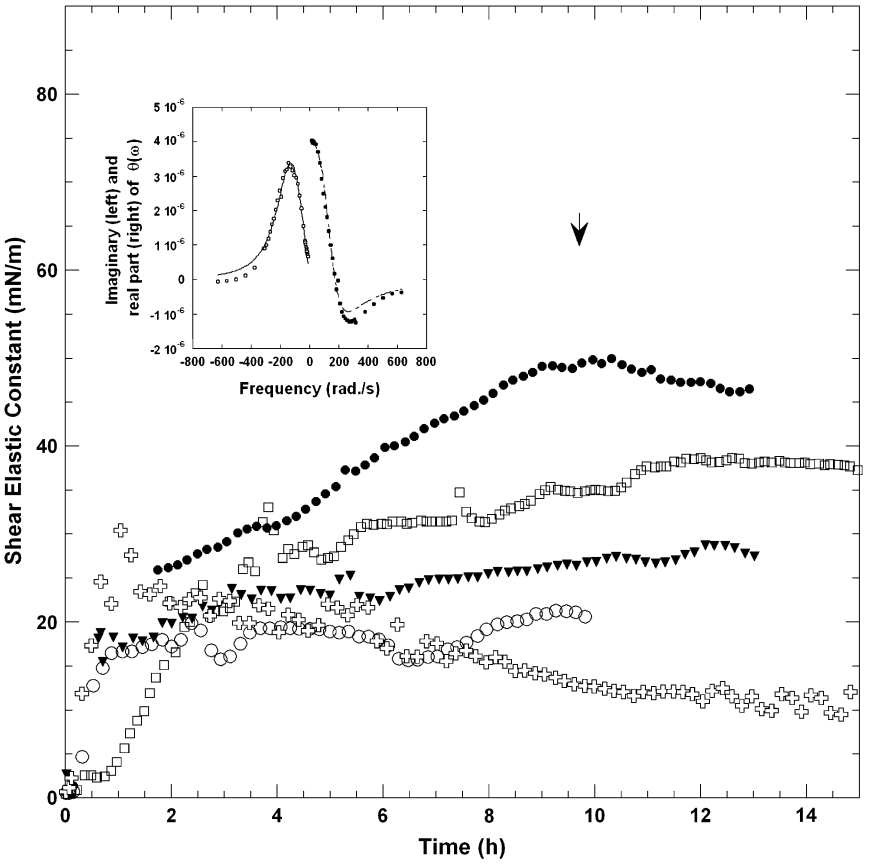

FIGURE 7 Shear elastic constant, μ, as a function of time of exchangeable apolipoproteins at the subphase concentration of 3 μg/ml. (*Open squares*) ApoC-I; (*open circles*) ApoA-I; (*solid circles*) ApoA-II; (*solid triangles*) ApoC-III; (*crosses*) ApoC-II. The end of the adsorption kinetics (~10 h) is indicated by the arrow. (*Inset*) The mechanical response of the layer at the end of the kinetic interval was recorded as a function of the pulsation ω. The imaginary and real parts of the response adjust well to a harmonic oscillator, indicating that the monolayer fits an elastic layer model. For clarity, the imaginary part has been plotted versus $-\omega$. The curves correspond to ApoA-I and are representative of the other exchangeable apolipoproteins.

TABLE 2 Values of μ^H/residue of amphipathic α-helical regions of exchangeable apolipoproteins

Protein	Number of residues/molecular mass (kDa)	PDB access No.	Residues involved in α-helix formation	μ^H/residue (kcal/mol)	μ^H_{avg} (kcal/mol)
ApoA-I	243/28.3	2A01	10–39	0.44	0.39
			50–83	0.43	
			97–116	0.45	
			121–137	0.39	
			146–187	0.28	
			196–213	0.38	
			219–241	0.31	
ApoA-II	77/8.7	1L6K	8–32	0.51	0.48
			56–71	0.45	
ApoC-I	57/6.6	1IOJ	13–25	0.51	0.49
			37–52	0.47	
ApoC-II	79/8.9	1SOH	14–35	0.45	0.35
			62–76	0.25	
ApoC-III	79/8.7	Structure model (22)	8–36	0.43	0.42
			41–71	0.41	

The interfacial maximal surface pressures of ApoA-I, ApoA-II, ApoC-I, ApoC-II, and ApoC-III are comparable to that of a de novo peptide ((PLAEELRARLRAQLEEL-RERLG)$_2$-NH$_2$) designed on the basis of the amino acid residue conservation of the amphipathic α-helices of ApoA-I, ApoA-IV, and ApoE (56). The putative apolipoprotein peptide showed a maximal surface pressure in the range 24 to 27 mN/m at the same concentration of 10^{-6} M. However, compared with this consensus sequence peptide, the exchangeable apolipoprotein ApoA-I proved to be more flexible at the interface (57), supporting the idea that flexibility and surface pressure-mediated desorption and readsorption of ApoA-I confer lipoprotein stability during metabolic remodeling reactions (57).

Although exchangeable apolipoproteins show a common rapid adsorption at interfaces and formed stable monolayers, important differences in the interfacial behavior of these proteins were noticed. For instance, when surface pressure has initiated ($\Gamma = \Gamma_0$), nearly two times more ApoA-I molecules than any other apolipoprotein were adsorbed at the interface until the condition where $\Gamma = 2.7\ \Gamma_0$, suggesting that once the first molecules adsorb at the interface (inducing a nonnull surface pressure) some surface remains available for the adsorption of additional molecules. In contrast, when lateral interactions were established between molecules in ApoA-II, ApoC-I, and ApoC-III monolayers, a few more molecules could be adsorbed at the interface ($\Gamma = 1.5\Gamma_0$). This observation correlates well with the relatively few conformational constraints of the latter group, which leads to the complete covering of the surface once these exchangeable apolipoproteins have sampled a larger conformational space.

The different adsorption kinetics of exchangeable apolipoproteins evidences the fundamental role of α-helix amphiphilicity in the determination of interfacial properties. Equation 2 shows that α-helix amphiphilicity can be estimated from the magnitude of the hydrophobic moment, μ^H (58), as follows:

$$\mu\mathrm{H} = 1/N\,[[\sum_{n=1} Hn \sin(\delta n)]^2 + [\sum_{n=1} Hn \cos(\delta n)]^2]^{1/2}, \quad (2)$$

where δn corresponds to the angle formed between amino acid lateral chains of two adjacent residues with respect to the plane of the α-helix (for an ideal α-helix, $\delta = 100°$); $N =$ the number of residues in that α-helix; and H_n, the numerical hydrophobicity of the nth residue, corresponds to a theoretical value of the degree of partition of an amino acid between the surface and the interior of a globular protein. α-Helical regions with μ^H values higher than 0.2 kcal/mol per residue are considered good amphipathic α-helices. As Table 2 shows, the first α-helix of ApoC-I (residues 13–25) exhibits a higher hydrophobic moment value ($\mu^H = 0.51$ kcal/mol per residue) than the second one (residues 37–52) ($\mu^H = 0.46$ kcal/mol per residue). The high amphiphilicity of the α-helix segments of ApoC-I explains how the smallest of the exchangeable apolipoproteins reported to date is able to displace a larger apolipoprotein molecule such as ApoE from β-VLDL particles (26). Similarly, the displacement of ApoA-I by ApoA-II from HDL particles (59) can be explained considering the higher average α-helix amphiphilicity ($\mu^H_{avg} = \mu^H_i/n_i$) of ApoA-II ($\mu^H_{avg}$ 0.48 kcal/mol per residue) compared with that of ApoA-I ($\mu^H_{avg} = 0.38$ kcal/mol per residue). Even though the high surface activity of exchangeable apolipoproteins is largely determined by the overall α-helix amphiphilicity, other properties such as self-association, which varies greatly among exchangeable apolipoproteins, may affect the rate at which these proteins move from the bulk toward the interface. For instance, in its lipid-bound conformation, ApoA-I can self-associate and form dimers in a process that involves intramolecular interactions between the N-terminal and C-terminal ends (60). Such self-association also seems to

account for the stable interaction of ApoA-I with HDL particles (60,61). We show that the maximal surface activity of ApoA-I and ApoA-II is comparable to that reported by others (ApoA-I, 22 mN/m (32); ApoA-II, 24 mN/m (32)) but differs significantly from the value described in other reports (ApoA-I, 32 mN/m (29); ApoA-II, 34 mN/m (62)). Overall, the discrepancy reflects the different conditions (pH, temperature, etc.,) in which the experiments were carried out. In the case of ApoC-I, ApoC-II, and ApoC-III, no comparison with other publications can be made because, to the best of our knowledge, this is the first report in which the interfacial behavior of the three human apolipoproteins is described.

A previous study on compressed monolayers of ApoA-II suggested that this apolipoprotein is predominantly stabilized at the air-water interface through short-range interactions (63). Clearly, the study of the evolution of μ as a function of time for ApoA-II and other exchangeable apolipoproteins (Fig. 7) challenged that notion. The discrepancy seems to originate from the technical limitations of the experimental setup described in that report. Indeed, Ruiz-Garcia et al. (63) noticed the contamination of transferred ApoA-II monolayers with potassium chloride crystals and recognized that AFM observations were difficult to interpret and led to inconsistent estimations of the unit cell dimensions. In contrast, our setup permits the monitoring of changes in the rheology of the protein at the interface without further manipulation of the system. The high magnitude of μ ($>$20 mN/m) with regard to the low bulk concentration (3 μg/ml) and the satisfactory fit to an elastic model strongly suggest the establishment of medium-range and long-range interactions between exchangeable apolipoproteins when they are deposited onto monolayers. Although we observed that ApoA-I, ApoA-II, ApoC-I, ApoC-II, and ApoC-III monolayers exhibit different evolution of the shear elastic constant, in all of the cases stable, relatively rigid films were formed after a few hours. Interestingly, medium- and long-range interactions are recognized to play an important role in the reshape of ApoA-I-containing lipoprotein particles from discoidal to spherical structures in vitro (64) and may contribute to the confinement of ApoA-II monomers to the circumference of discoidal lipoprotein particles in vivo (65). Moreover, the conformational constraints of adjacent amphipathic α-helices of ApoA-I Milano imposed by these classes of interactions seem to explain the fact that this isoform is twice as effective as ApoA-I Paris in protecting phospholipids from oxidation (66).

These observations suggest that some of the physicochemical parameters that govern the behavior of apolipoprotein monolayers influence protein function. Independent studies on ApoA-I and ApoA-II have shown that the stoichiometry of displacement of ApoA-I by ApoA-II at flat lipid monolayers spread at the air-water interface and at the surfaces of HDL and lipid-protein complexes is similar (33,67). However, rheological measurements on ApoA-I adsorbed under lipidic layers have demonstrated that the presence of ApoA-I in a lipidic layer does not increase the rigidity of the latter, suggesting that this apolipoprotein does not establish the same long-range interactions in the presence of lipids as it does at the air-water interface (S. Beaufils, V. M. Bolanos-Garcia, and M. Pinot, unpublished results). Thermal denaturation and far-UV CD spectroscopy on several exchangeable apolipoproteins associated with HDL particles have shown that such association decelerates protein unfolding by at least 10 orders of magnitude compared with the lipid-free form (39). In addition, it seems that the molecular determinants of the stability of exchangeable apolipoproteins under physiological conditions and those of monolayers of isolated proteins might be different and likely to involve high kinetic barriers (39). Hence, the study of lipid-free exchangeable apolipoproteins deposited onto monolayers is insufficient to fully describe the behavior observed under physiological conditions. Nevertheless, the characterization of the surface rheology of monolayers of exchangeable apolipoproteins supports the idea that medium-range and long-range interactions are the main stabilizing forces in all α-helix proteins compared with those involved in the stabilization of the structural classes all-β, $\alpha+\beta$, and α/β (68). Surface rheology measurements show that monolayers of exchangeable apolipoproteins are comparably less rigid than those of the TPR motifs of PP5 and BUBR-1, which is in good agreement with the lower conformational constraints of the former group and their hallmark property of exchange between lipoprotein particles.

Our study provides insights into the adsorption kinetics, surface activity, and rheology of exchangeable apolipoproteins and the relation between these properties and their physiological functions. We also show the importance of medium-range and long-range interactions among amphipathic α-helix segments for the stability of these proteins at air-water interfaces. Further insight into the nature of medium- and long-range interactions between proteins in the interfacial layer could be brought by PM-IRRAS experiments, giving information on the conformation of proteins at the interface during their adsorption and once the layer is formed. Such studies are currently in progress. Because it will be particularly important to generate information on the interfacial properties of exchangeable apolipoproteins in the lipid-bound state, future work will seek to study ApoA-I, ApoA-II, ApoCI, ApoC-II, and ApoC-III deposited onto lipid-water monolayers.

We are grateful to Mr. Lionel Chieze for providing us with unpublished data on the surface pressure of apoA-I at various subphase concentrations and to Prof. C. Salesse for critical reading of the manuscript. The comments and suggestions of anonymous referees are also appreciated.

REFERENCES

1. Fielding, C., and P. Fielding. 1995. Molecular physiology of reverse cholesterol transport. *J. Lipid Res.* 36:211–228.
2. Liu, T., M. Krieger, H.-Y. Kan, and V. I. Zannis. 2002. The effects of mutations in helices 4 and 6 of ApoA-I on scavenger receptor class b type i (sr-bi)-mediated cholesterol efflux suggest that formation of a productive complex between reconstituted high density lipoprotein and

sr-bi is required for efficient lipid transport. *J. Biol. Chem.* 277:21576–21584.

3. Arakawa, R., and S. Yokoyama. 2002. Helical apolipoproteins stabilize ATP-binding cassette transporter A1 by protecting it from thiol protease-mediated degradation. *J. Biol. Chem.* 277:22426–22429.
4. Major, A. S., D. E. Dove, H. Ishiguro, Y. R. Su, A. M. Brown, L. Liu, K. J. Carter, M. F. Linton, and S. Fazio. 2001. Increased cholesterol efflux in apolipoprotein AI (ApoAI)-producing macrophages as a mechanism for reduced atherosclerosis in ApoAI(−/−) mice. *Arterioscler. Thromb. Vasc. Biol.* 21:1790–1795.
5. Nishida, H., T. Nakanishi, E. Yen, H. Arai, F. Yen, and T. Nishida. 1986. Nature of the enhancement of lecithin-cholesterol acyltransferase reaction by various apolipoproteins. *J. Biol. Chem.* 261:12028–12035.
6. Vadiveloo, P. K., C. M. Allan, B. J. Murray, and N. H. Fidge. 1993. Interaction of apolipoprotein AII with the putative high-density lipoprotein receptor. *Biochemistry.* 32:9480–9485.
7. Sprecher, D., L. Taam, and H. Brewer, Jr. 1984. Two-dimensional electrophoresis of human plasma apolipoproteins. *Clin. Chem.* 30:2084–2092.
8. Furlaneto, C. J., F. P. Ribeiro, E. Hatanaka, G. M. Souza, M. A. Cassatella, and A. Campa. 2002. Apolipoproteins A-I and A-II down-regulate neutrophil functions. *Lipids.* 37:925–928.
9. Ribas, V., J. L. Sanchez-Quesada, R. Anton, M. Camacho, J. Julve, J. C. Escola-Gil, L. Vila, J. Ordonez-Llanos, and F. BlancoVaca. 2004. Human apolipoprotein A-II enrichment displaces paraoxonase from HDL and impairs its antioxidant properties: a new mechanism linking HDL protein composition and antiatherogenic potential. *Circ. Res.* 95: 789–797.
10. Malik, G., M. D. Ward, S. K. Gupta, M. W. Trosset, W. E. Grizzle, B.-L. Adam, J. I. Diaz, and O. J. Semmes. 2005. Serum levels of an isoform of apolipoprotein A-II as a potential marker for prostate cancer. *Clin. Cancer Res.* 11:1073–1085.
11. Yazaki, M., J. J. Liepnieks, T. Yamashita, B. Guenther, M. Skinner, and M. D. Benson. 2001. Renal amyloidosis caused by a novel stop-codon mutation in the apolipoprotein A-II gene. *Kidney Int.* 60:1658–1665.
12. Gautier, T., D. Masson, J.-P. P. De Barros, A. Athias, P. Gambert, D. Aunis, M.-H. Metz-Boutigue, and L. Lagrost. 2000. Human apolipoprotein C–I accounts for the ability of plasma high density lipoproteins to inhibit the cholesteryl ester transfer protein activity. *J. Biol. Chem.* 275:37504–37509.
13. Petit-Turcotte, C., S. M. Stohl, U. Beffert, J. S. Cohn, N. Aumont, M. Tremblay, D. Dea, L. Yang, J. Poirier, and N. S. Shachter. 2001. Apolipoprotein C–I expression in the brain in Alzheimer's disease. *Neurobiol. Dis.* 8:953–963.
14. Serra-Grabulosa, J. M., P. Salgado-Pineda, C. Junqué, C. Solé-Padullés, P. Moral, A. López-Alomar, T. López, A. López-Guillén, N. Bargalló, J. M. Mercader, I. C. Clemente, and D. Bartrés-Faz. 2003. Apolipoproteins E and C1 and brain morphology in memory impaired elders. *Neurogenetics.* 4:141–146.
15. Jong, M. C., P. J. Voshol, M. Muurling, V. E. H. Dahlmans, J. A. Romijn, H. Pijl, and L. M. Havekes. 2001. Protection from obesity and insulin resistance in mice overexpressing human apolipoprotein C1. *Diabetes.* 50:2779–2785.
16. Kolmakova, A., P. Kwiterovich, D. Virgil, P. Alaupovic, C. Knight-Gibson, S. F. Martin, and S. Chatterjee. 2004. Apolipoprotein C–I induces apoptosis in human aortic smooth muscle cells via recruiting neutral sphingomyelinase. *Arterioscler. Thromb. Vasc. Biol.* 24:264–269.
17. Conde-Knape, K., A. Bensadoun, J. H. Sobel, J. S. Cohn, and N. S. Shachter. 2002. Overexpression of apoC-I in apoE-null mice: severe hypertriglyceridemia due to inhibition of hepatic lipase. *J. Lipid Res.* 43: 2136–2145.
18. Zdunek, J., G. V. Martinez, J. Schleucher, P. O. Lycksell, Y. Yin, S. Nilsson, Y. Shen, G. Olivecrona, and S. Wijmenga. 2003. Global structure and dynamics of human apolipoprotein CII in complex with micelles: evidence for increased mobility of the helix involved in the activation of lipoprotein lipase. *Biochemistry.* 42:1872–1889.
19. Sparks, D., and P. Pritchard. 1989. Transfer of cholesteryl ester into high density lipoprotein by cholesteryl ester transfer protein: effect of HDL lipid and apoprotein content. *J. Lipid Res.* 30:1491–1498.
20. Cohn, S., M. Tremblay, R. Batal, C. Jacques, G. Rodriguez, O. Mamer, and J. Davignon. 2004. Increased apoC-III production is a characteristic feature of patients with hypertriglyceridemia. *Atherosclerosis.* 177: 137–145.
21. Juntti-Berggren, L., E. Refai, I. Appelskog, M. Andersson, G. Imreh, N. Dekki, S. Uhles, L. Yu, W. J. Griffiths, S. Zaitsev, and others. 2004. Apolipoprotein CIII promotes Ca^{2+}-dependent {beta} cell death in type 1 diabetes. *Proc. Natl. Acad. Sci. USA.* 101:10090–10094.
22. Bolanos-Garcia, V. M., and R. N. Miguel. 2003. On the structure and function of apolipoproteins: more than a family of lipid-binding proteins. *Prog. Biophys. Mol. Biol.* 83:47–68.
23. Sun, G., N. Bi, G. Li, X. Zhu, W. Zeng, G. Wu, H. Xue, and B. Chen. 2006. Identification of lipid binding and lipoprotein lipase activation domains of human apoAV. *Chem. Phys. Lipids.* 143:22–28.
24. Dumont, L., T. Gautier, J.-P. P. De Barros, H. Laplanche, D. Blache, P. Ducoroy, J. Fruchart, J.-C. Fruchart, P. Gambert, D. Masson, and L. Lagrost. 2005. Molecular mechanism of the blockade of plasma cholesteryl ester transfer protein by its physiological inhibitor apolipoprotein CI. *J. Biol. Chem.* 280:38108–38116.
25. Perez-Mendez, O., E. Bruckert, G. Franceschini, N. Duhal, B. Lacroix, J. P. Bonte, C. Sirtori, J. C. Fruchart, G. Turpin, and G. Luc. 2000. Metabolism of apolipoproteins AI and AII in subjects carrying similar apoAI mutations, apoAI Milano and apoAI Paris. *Atherosclerosis.* 148:317–325.
26. Swaney, J., and K. Weisgraber. 1994. Effect of apolipoprotein C–I peptides on the apolipoprotein E content and receptor-binding properties of β-migrating very low density lipoproteins. *J. Lipid Res.* 35: 134–142.
27. Clavey, V., S. Lestavel-Delattre, C. Copin, J. M. Bard, and J. C. Fruchart. 1995. Modulation of lipoprotein B binding to the LDL receptor by exogenous lipids and apolipoproteins CI, CII, CIII, and E. *Arterioscler. Thromb. Vasc. Biol.* 15:963–971.
28. Lins, L., C. Flore, L. Chapelle, P. J. Talmud, A. Thomas, and R. Brasseur. 2002. Lipid-interacting properties of the N-terminal domain of human apolipoprotein C–III. *Protein Eng.* 15:513–520.
29. Weinberg, R. B., R. A. Anderson, V. R. Cook, F. Emmanuel, P. Denefle, A. R. Tall, and A. Steinmetz. 2002. Interfacial exclusion pressure determines the ability of apolipoprotein A-IV truncation mutants to activate cholesterol ester transfer protein. *J. Biol. Chem.* 277:21549–21553.
30. Bolanos-Garcia, V. M., J. Mas-Oliva, S. Ramos, and R. Castillo. 1999. Phase transitions in monolayers of human apolipoprotein C–I. *J. Phys. Chem. B.* 103:6236–6242.
31. Bolanos-Garcia, V. M., S. Ramos, R. Castillo, J. Xicohtencatl-Cortes, and J. Mas-Oliva. 2001. Monolayers of apolipoproteins at the air/water interface. *J. Phys. Chem. B.* 105:5757–5765.
32. Krebs, K. E., J. A. Ibdah, and J. C. Phillips. 1988. A comparison of the surface activities of human apolipoproteins A-I and A-II at the air-water interface. *Biochim. Biophys. Acta.* 959:229–237.
33. Ibdah, J. A., K. E. Krebs, and J. C. Phillips. 1989. The surface properties of apolipoproteins A-I and A-II at the lipid/water interface. *Biochim. Biophys. Acta.* 1004:300–308.
34. Berge, B., and A. Renault. 1993. Ellipsometry study of 2D crystallization of 1-alcohol monolayers at the water surface. *Europhys. Lett.* 21:773–777.
35. Azzam, R. M. A., and N. M. Bashara. 1977. Ellipsometry and polarized light. *In* North Holland Personal Library. Amsterdam. p. 340.
36. De Feijter, J. A., J. Benjamins, and F. A. Veer. 1978. Ellipsometry as a tool to study the adsorption behavior of synthetic and biopolymers at the air-water interface. *Biopolymers.* 17:1759–1772.
37. Venien-Bryan, C., P.-F. Lenne, C. Zakri, A. Renault, A. Brisson, J.-F. Legrand, and B. Berge. 1998. Characterization of the growth of 2D protein crystals on a lipid monolayer by ellipsometry and rigidity measurements coupled to electron microscopy. *Biophys. J.* 74:2649–2657.

38. Renault, A., P.-F. Lenne, C. Zakri, A. Aradian, C. Venien-Bryan, and F. Amblard. 1999. Surface-induced polymerization of actin. *Biophys. J.* 76:1580–1590.

39. Jayaraman, S., D. L. Gantz, and O. Gursky. 2005. Kinetic stabilisation and fusion of apolipoprotein A-2:DMPC disks: comparison with apoA-1 and ApoC-1. *Biophys. J.* 68:2907–2918.

40. Donovan, J. M., G. B. Benedek, and M. C. Carey. 1987. Self-assiciation of human apolipoproteins A-I and A-II and interactions of apolipoprotein A-I with bile salts: quasi-elastic light scattering studies. *Biochemistry.* 26:8116–8125.

41. Bolanos-Garcia, V. M., J. Mas-Oliva, and A. Moreno. 1998. Pre-crystallisation of human apoprotein A-I based on its aggregation behavior in solution studied by dynamic light scattering. *J. Mol. Struct.* 440:1–8.

42. Bolanos-Garcia, V. M., S. Beaufils, A. Renault, J. G. Grossmann, S. Brewerton, M. Lee, A. Venkitaraman, and T. L. Blundell. 2005. The conserved N-terminal region of the mitotic checkpoint protein BUBR1: a putative TPR motif of high surface activity. *Biophys. J.* 89: 2640–2649.

43. Graham, D. E., and M. C. Phillips. 1979. Proteins at liquid interfaces 2. adsorption isotherms. *J. Colloid Interface Sci.* 70:415–426.

44. Graham, D. E., and M. C. Phillips. 1979. Proteins at liquid interfaces 3. molecular structures of adsorbed films. *J. Colloid Interface Sci.* 70:427–439.

45. Damodaran, S. and C. S. Rao. 2001. Molecular basis for protein adsorption at fluid-fluid interfaces. *In* Food colloids: fundamental of formulation. E. Dickinson and R. Miller, editors. Royal Society of Chemistry, London. p. 165–180.

46. Beaufils, S., R. Hadaoui-Hammoutene, V. Vie, G. Miranda, J. Perez, E. Terriac, G. Henry, M.-M. Delage, J. Leonil, P. Martin, and A. Renault. 2007. Comparative behaviour of goat [β] and [α]s1-caseins at the air-water interface and in solution. *Food Hydrocolloids.* 21:1330–1343.

47. Ward, A. F., and L. Tordai. 1946. Time dependance of boundary tensions of solutions. I. The role of diffusion in time effects. *J. Chem. Phys.* 14:453–461.

48. Campos-Teran, J., J. Mas-Oliva, and R. Castillo. 2004. Interactions and conformations of alpha-helical human apolipoprotein CI on hydrophilic and on hydrophobic substrates. *J. Phys. Chem. B.* 108:20442–20450.

49. Davidson, W. S., and G. D. Silva. 2005. Apolipoproteins structural organization in high-density lipoproteins: belts, bundles, hinges and hairpins. *Curr. Opin. Lipidol.* 16:295–300.

50. Brouillette, C. G., W.-J. Dong, Z. W. Yang, M. J. Ray, I. I. Protasevich, H. C. Cheung, and J. A. Engler. 2005. Forster resonance energy transfer measurements are consistent with a helical bundle model for lipid-free apolipoprotein A-I. *Biochemistry.* 44:16413–16425.

51. Borhani, D. W., D. P. Rogers, J. A. Engler, and C. G. Brouillette. 1997. Crystal structure of truncated human apolipoprotein A-I suggests a lipid-bound conformation. *Proc. Natl. Acad. Sci. USA.* 94:12291–12296.

52. Kumar, M. S., M. Carson, M. M. Hussain, and H. M. K. Murthy. 2002. Structures of apolipoprotein A-II and a lipid-surrogate complex provide insights into apolipoprotein-lipid interactions. *Biochemistry.* 41:11681–11691.

53. Rozek, A., J. T. Sparrow, K. H. Weisgraber, and R. J. Cushley. 1998. Sequence-specific 1H NMR resonance assignments and secondary structure of human apolipoprotein C–I in the presence of sodium dodecyl sulfate. *Biochem. Cell Biol.* 76:267–275.

54. Mac Raild, C. A., D. M. Hatters, G. J. Howlett, and P. R. Gooley. 2001. NMR structure of human apolipoprotein C–II in the presence of sodium dodecyl sulfate. *Biochemistry.* 40:5414–5421.

55. Saito, H., P. Dhanasekaran, D. Nguyen, E. Deridder, P. Holvoet, S. Lund-Katz, and M. C. Phillips. 2004. $\{\alpha\}$-Helix formation is required for high affinity binding of human apolipoprotein A-I to lipids. *J. Biol. Chem.* 279:20974–20981.

56. Wang, L., D. Atkinson, and D. M. Small. 2003. Interfacial properties of an amphipathic $\{\alpha\}$-helix consensus peptide of exchangeable apolipoproteins at air/water and oil/water interfaces. *J. Biol. Chem.* 278: 37480–37491.

57. Wang, L., D. Atkinson, and D. M. Small. 2005. The Interfacial Properties of ApoA-I and an Amphipathic $\{\alpha\}$-helix consensus peptide of exchangeable apolipoproteins at the triolein/water interface. *J. Biol. Chem.* 280:4154–4165.

58. Eisenberg, D., R. M. Weiss, and T. C. Terwilliger. 1982. The helical hydrophobic moment: a measure of the amphiphilicity of a helix. *Nature.* 299:371–374.

59. Durbin, D. M., and A. Jonas. 1997. The effect of apolipoprotein A-II on the structure and function of apolipoprotein A-I in a homogeneous reconstituted high density lipoprotein particle. *J. Biol. Chem.* 272: 31333–31339.

60. Bhat, S., M. G. Sorci-Thomas, E. T. Alexander, M. P. Samuel, and M. J. Thomas. 2005. Intermolecular contact between globular N-terminal fold and C-terminal domain of ApoA-I stabilizes its lipid-bound conformation: studies employing chemical cross-linking and mass spectrometry. *J. Biol. Chem.* 280:33015–33025.

61. Gross, E., P. D. Qeng, S. L. Hazen, and J. D. Smith. 2006. A novel folding intermediate state for apolipoprotein A-I: role of the amino and carboxy termini. *Biophys. J.* 90:1362–1370.

62. Phillips, M. C., and K. E. Krebs. 1986. Studies of apolipoproteins at the air-water interface. *Methods Enzymol.* 128:387–403.

63. Ruiz-Garcia, J., A. Moreno, G. Brezesinski, H. Mohwald, J. Mas-Oliva, and R. Castillo. 2003. Phase transitions and conformational changes in monolayers of human apolipoproteins CI and AII. *J. Phys. Chem. B.* 107: 11117–11124.

64. Rogers, D. P., L. M. Roberts, J. Lebowitz, G. Datta, G. M. Anantharamaiah, J. A. Engler, and C. G. Brouillette. 1998. The lipid-free structure of apolipoprotein A-I: effects of amino-terminal deletions. *Biochemistry.* 37:11714–11725.

65. Clay, M. A., D. H. Pyle, K.-A. Rye, and P. J. Barter. 2000. Formation of spherical, reconstituted high density lipoproteins containing both apolipoproteins A-I and A-II is mediated by lecithin:cholesterol acyltransferase. *J. Biol. Chem.* 275:9019–9025.

66. Bielicki, J. K., and M. N. Oda. 2002. Apolipoprotein A-IMilano and apolipoprotein A-IParis exhibit an antioxidant activity distinct from that of wild-type apolipoprotein A-I. *Biochemistry.* 41:2089–2096.

67. Lagocki, P., and A. Scanu. 1980. In vitro modulation of the apolipoprotein composition of HDL. Displacement of apolipoprotein A-I from HDL by apolipoprotein A-II. *J. Biol. Chem.* 255:3701–3706.

68. Gromiha, M. M., and S. Selvaraj. 2004. Inter-residue interactions in protein folding and stability. *Prog. Biophys. Mol. Biol.* 86:235–277.